SCIENCE CHINA
Information Sciences

• LETTER •

December 2020, Vol. 63 229401:1–229401:3
https://doi.org/10.1007/s11432-019-2700-1

High-quality and large-grain epi-like Si film by $NiSi_2$-seed initiated lateral epitaxial crystallization (SILEC)

Yuancheng YANG, Baotong ZHANG, Xiaoqiao DONG, Xiaokang LI, Shuang SUN, Qifeng CAI, Ran BI, Xiaoyan XU, Ming LI* & Ru HUANG

Key Laboratory of Microelectronic Devices and Circuits, Institute of Microelectronics, Peking University, Beijing 100871, China

Received 9 September 2019/Revised 27 October 2019/Accepted 9 November 2019/Published online 28 June 2020

Citation Yang Y C, Zhang B T, Dong X Q, et al. High-quality and large-grain epi-like Si film by $NiSi_2$-seed initiated lateral epitaxial crystallization (SILEC). Sci China Inf Sci, 2020, 63(12): 229401, https://doi.org/10.1007/s11432-019-2700-1

Dear editor,

Three-dimensional monolithic integration (3D-MI) has recently emerged for both "more Moore" and "more than Moore" applications, because of its high integration density, high bandwidth and multi-functions [1]. With 3D-MI, different types of devices can be stacked on the same platform and in a single process flow. A critical issue for 3D-MI is the formation of high-quality channels for the devices on the upper level under the constraints of low thermal budget and low cost. Several efforts have been reported to realize poly-Si thin film channels on SiO_2 at low temperature, for example, laser annealing (LA) [2], solid phase crystallization (SPC) [3], and metal-induced lateral crystallization (MILC) [4]. LA can obtain a single-crystal-like thin film, but needs extraordinary atomic-level chemical-mechanical polishing (CMP) to reduce surface roughness, which results in high process variation and cost. SPC is a common and simple technique, but its crystallization rate is too slow to efficiently form the active layer, and the random self-nucleation mechanism can lead to large fluctuations in grain size. MILC is another cost-effective method that can improve the crystallization rate, but suffers from serious metal contamination and a large number of dislocation defects in silicon grains because of metal-silicon inter-diffusion.

In this study, a novel crystallization technique using low-temperature $NiSi_2$-seed initiated lateral epitaxial crystallization ($NiSi_2$-SILEC) is proposed. Using this technique, we perform an experimental demonstration, in which a 1-nm-thick Al_2O_3 layer is used to modify Ni diffusion and $NiSi_2$ seed formation. The {111} facets of $NiSi_2$ act as the initial seed window for silicon solid-phase epitaxy. Additionally, a two-step annealing scheme is adopted to separate the two processes: $NiSi_2$ formation and silicon epitaxial crystallization. Finally, the mechanism of $NiSi_2$-SILEC is discussed in detail.

Experiment. Three crystallization schemes are compared: SILEC, MILC and SPC. All the samples start from a bulk silicon substrate with a 100-nm thermal oxide layer. A 40-nm amorphous silicon (α-Si) film is deposited by low pressure chemical vapor deposition (LPCVD) at 425°C. Then, the α-Si layer is patterned to a dumbbell-shaped structure, which comprises a 10 μm × 4 μm bar and two 17 μm × 24 μm fan-out pads. The natural oxide layer on the α-Si surface is stripped by dilute hydrofluoric acid solution. For SILEC only, a 1-nm Al_2O_3 is grown as a Ni diffusion barrier by plasma enhanced atomic layer deposi-

* Corresponding author (email: liming.ime@pku.edu.cn)

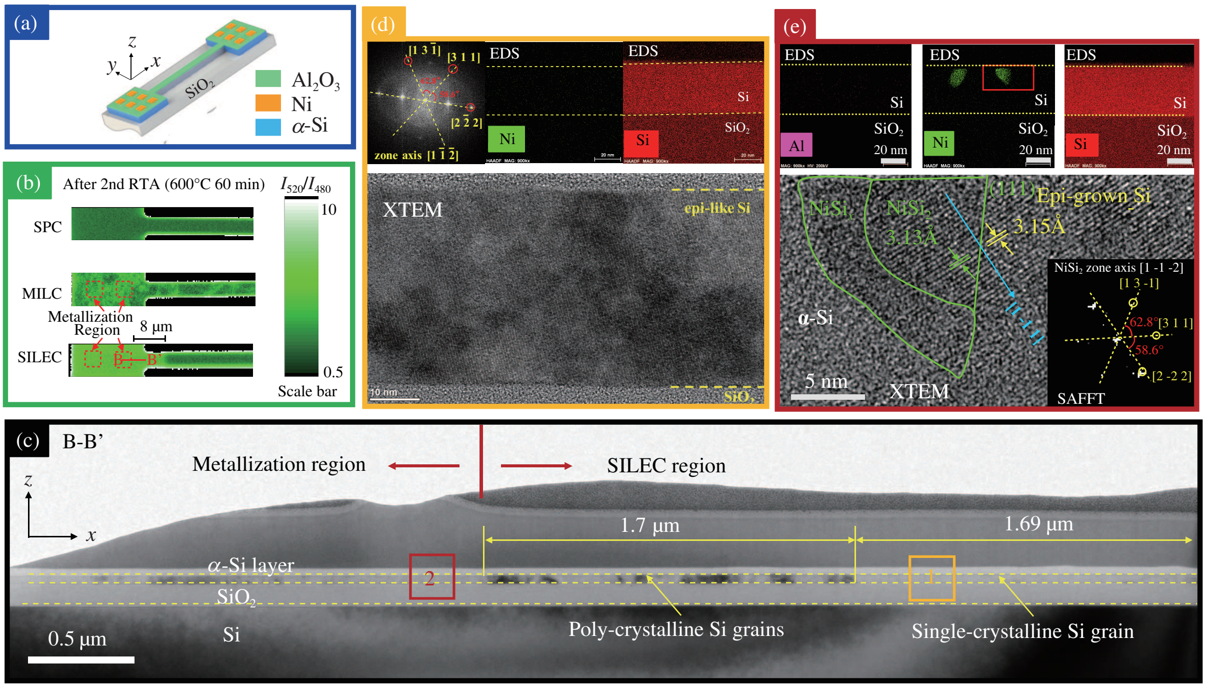

Figure 1 (Color online) (a) Schematic of the SILEC sample after Ni pads patterning; (b) micro-Raman mapping of SPC, MILC, and SILEC samples (only the left half of the dumbbell-shaped structure is shown); (c) low magnification cross-sectional transmission electron microscope (XTEM) image of the SILEC sample cut off along B-B' in (b) by focused ion beam (FIB); (d) high magnification XTEM, selected area fast Fourier transform (SAFFT) and energy dispersive X-ray (EDX) mapping at the region marked as "1" in (c); (e) high magnification XTEM, SAFFT and EDX mapping at the region marked as "2" in (c).

tion (PEALD). Subsequently, a 50-nm Ni film is deposited by direct current sputtering at 300 W, and then patterned into a 3 × 2 array of 4 μm × 4 μm pads as the metallization source on the fan-out pads by lift-off, for both SILEC (see Figure 1(a)) and MILC. The SPC sample skips the Al_2O_3 and the Ni deposition processes. Finally, all the samples underwent a two-step annealing in N_2 ambient: the first annealing at 600°C for 10 min (Note that for SILEC and MILC, the unreacted Ni pads are stripped by H_2SO_4-H_2O_2 solution after the first annealing) and the second annealing at 600°C for 1 h.

Results and discussion. Figure 1(b) shows the micro-Raman mapping of the three groups of samples after the second annealing. For Raman spectrum of silicon, a flat plateau at approximately 480 cm^{-1} corresponds the transverse optical (TO) mode vibration of amorphous Si-Si bonds, while the peak at 520 cm^{-1} corresponds the TO mode vibration of single-crystalline Si-Si bonds [5]. Therefore, the ratio of the intensity at 520 cm^{-1} to that at 480 cm^{-1} can semi-quantitatively reflect the crystallization degree. In this experiment, SPC does not occur during the 1-hour annealing at 600°C and MILC generates a crystalline/amorphous-mixed region composed of separated, randomly distributed and low-degree-crystalline sub-regions. In contrast, SILEC shows a uniform and intact lateral crystallized region with a length up to 8 μm from the edge of the metallization region and a clear amorphous/crystalline interface.

Figure 1(c) shows the cross-sectional transmission electron microscope (XTEM) image of the SILEC sample cuts off along X-axis (B-B' in Figure 1(b) by focused ion beam (FIB). The lateral crystallization region comprises two parts: a 1.7-μm-long poly-crystalline subregion at the edge of the metallization region and a single-crystalline subregion adjacent to such a poly-crystalline subregion. The poly-crystalline subregion contains about 10 grains with a mean size of 216 nm. In contrast, the length of the single-crystalline subregion is up to 1.69 μm. Emphasis must be placed on the fact that obtaining the whole lateral crystallization region by FIB is difficult, but the fact that the length of the single-crystalline region is more than 1.69 μm can be inferred, and the lateral crystallization region can be almost single-crystalline. Figure 1(d) identifies this crystalline silicon grain (marked as "1" in Figure 1(c)) with orientations of [1 $\bar{1}$ 1], [3 1 1], and [1 3 $\bar{1}$] in X-Z plane. No amorphous regions or mis-oriented grains are found, which are usually caused by Ni atoms migration [6]. Additionally, the element signal of Ni is not detected in the crystalline silicon grain by energy dispersive X-ray (EDX) mapping whose elemental sensitivity is about 0.5 at.% (5 $\times$ 10^{21} cm^{-3}), indicating that the lateral diffusion of Ni is totally suppressed during the two-step annealing.

Figure 1(e) illustrates that the high-integrity lateral crystalline grains initiate from the {111} facets of $NiSi_2$ located in the metallization region (marked as "2" in Figure 1(c)). Confirmation is received that crystalline $NiSi_2$ and its adjacent Si grain have the same orientations as [1 $\bar{1}$ 1], [3 1 1] and [1 3 $\bar{1}$] in the X-Z plane. The interface between $NiSi_2$ and the silicon grain is another {111} facet that is not perpendicular to the X-Z plane. What is more, no cavity is observed in the metallization region, which indicate that $NiSi_2$ neither decomposes nor migrates out of the metallization region during the second annealing [7] because of the high thermal stability of $NiSi_2$ at 600°C.

The above analysis reveals a new crystallization mechanism in which SILEC is different from MILC. For MILC, Ni atoms move forward into α-Si and leave a one-dimensional (1D) needle-like Si crystallite behind. Locally, Ni-Si atom interchange occurs at the crystalline/amorphous interface. If the annealing time is not enough (e.g., 1 h in this experiment), such needles will not merge so that two-dimensional (2D) crystallization will not happen [6]. For SILEC, however, the Al_2O_3 barrier can effectively limit the amount of Ni atoms diffused into the α-Si layer and establishes a Si-rich mixed layer just beneath the Al_2O_3 barrier. As a result, the further Ni accumulation can be inhibited, and $NiSi_2$ will preferentially form during the first annealing. As the second annealing is carried out, the {111} facets of $NiSi_2$ grains will act as the initial seed planes for silicon atoms to reconstruct lattice. In this procedure, only silicon atoms migrate from the amorphous region to the $NiSi_2$ {111} surfaces. Therefore, the epitaxial growth of silicon {111} planes will start from the $NiSi_2$ {111} surfaces and expand layer by layer towards the amorphous region, with a 2D epitaxial crystallization mode. Emphasis should be placed on the fact that only the silicon atoms in contact with the crystalline $NiSi_2$ {111} facets can be transformed into crystalline phase, while the α-Si around amorphous $NiSi_x$ (see Figure 1(e)) remains amorphous.

Conclusion. In this study, a novel $NiSi_2$-seed initiated lateral epitaxial crystallization (SILEC) technique is proposed and experimentally verified. A 1-nm Al_2O_3 barrier layer inserted between Ni and α-Si can modulate Ni diffusion, and thus, $NiSi_2$ seeds can be formed beneath the Al_2O_3 barrier layer. The {111} facets of $NiSi_2$ grains will act as an initial seed planes to induce 2D silicon epitaxial recrystallization. Such silicon epitaxial growth process is separated from the $NiSi_2$ seed formation process by a two-step annealing scheme, which avoid potential metal contamination. By this method, large lateral epitaxial grown crystalline regions with up to 8-μm length can be obtained, which can be suitable as channel materials of the upper device in 3D monolithic integration in the future.

Acknowledgements This work was supported in part by National 02 Major Project (Grant No. 2017ZX02315-001-004), National Key Research and Development Plan (Grant No. 2016YFA0200504), Program of National Natural Science Foundation of China (Grant No. 61421005), and the 111 Project (Grant No. B18001).

References

1 Batude P, Brunet L, Fenouillet-Beranger C, et al. 3D sequential integration: application-driven technological achievements and guidelines. In: Proceedings of IEEE International Electron Devices Meeting, San Francisco, 2017. 1–3
2 Yang C, Shieh J, Hsieh T, et al. Footprint-efficient and power-saving monolithic IoT 3D+ IC constructed by BEOL-compatible sub-10nm high aspect ratio (AR>7) single-grained Si FinFETs with record high Ion of 0.38 mA/μm and steep-swing of 65 mV/dec. and Ion/Ioff ratio of 8. In: Proceedings of IEEE International Electron Devices Meeting, San Francisco, 2016. 1–9
3 Lu Y, Kuo P, Wu Y, et al. Novel GAA raised source/drain sub-10-nm poly-Si NW channel TFTs with self-aligned corked gate structure for 3-D IC applications. In: Proceedings of Symposium on VLSI Technology, Honolulu, 2011. 142–143
4 Su C J, Lin H C, Huang T Y. High-performance TFTs with Si nanowire channels enhanced by metal-induced lateral crystallization. IEEE Electron Device Lett, 2006, 27: 582–584
5 Duan C Y, Liu C, Ai B, et al. Selected area laser-crystallized polycrystalline silicon thin films by a pulsed Nd:YAG laser with 355 nm wavelength. J Semicond, 2011, 32: 123002
6 Miyasaka M, Makihira K, Asano T, et al. In situ observation of nickel metal-induced lateral crystallization of amorphous silicon thin films. Appl Phys Lett, 2002, 80: 944–946
7 Byun C W, Son S W, Lee Y W, et al. High performance poly-Si thin film transistors fabricated by a simple crystallization method using Ni-Silicide seeds. J Electrochem Soc, 2011, 158: 354–358